COUPLED HYDRO-MECHANICAL PROCESSES IN CRYTALLINE ROCK AND IN INDURATED AND PLASTIC CLAYS: A COMPARATIVE DISCUSSION

Chin-Fu Tsang[1], Peter Blümling[2] and Frederic Bernier[3]
[1]Lawrence Berkeley National Laboratory (LBNL, USA)
[2]Nationale Genossenschaft fur die Lagerung Radioaktiver Abfalle (NAGRA, Switzerland)
[3]European Underground Research Infrastructure for Disposal of Nuclear Waste in Clay Environment (EURIDICE, Belgium)

Abstract: This paper provides a comparative discussion of coupled hydromechanical processes in three different geological formations: crystalline rock, plastic clay, and indurated clay. First, the important processes and associated property characteristics in the three rock types are discussed. Then, one particular hydromechanical coupling is brought up for detailed consideration, that of pore pressure changes in nearby rock during tunnel excavation. Three field experiments in the three rock types are presented and their results are discussed. It is shown that the main physical processes are common to all three rock types, but with very different time constants. The different issues raised by these cases are pointed out, and the transferable lessons learned are identified. Such cross fertilization and simultaneous understanding of coupled processes in three very different rock types help to greatly enhance confidence in the state of science in this field.

1. INTRODUCTION

Coupled hydromechanical processes in geological formations are of much interest in nuclear waste disposal studies, tunnel construction, and slope stability. They operate when mechanical changes in rocks cause changes in hydraulic properties and flow conditions, and vice versa.

An important example is the so-called excavation damaged zone (EDZ) problem in construction of an underground nuclear waste repository. The creation of an EDZ is expected for all man-made openings in geologic formations, because of excavation procedure and associated stress redistribution. Macro- and microfracturing, and in general a rearrangement of rock structures, will occur in this zone, and may cause drastic increases of permeability to flow, mainly through the fractures or cracks induced by the excavation. The implications of such a high permeability zone in different disposal formations and its time evolution under various repository scenarios are being evaluated as part of waste repository safety assessment in a number of countries. Among formations being considered are crystalline hard rock, plastic or soft clays, and indurated or brittle claystones.

The present paper focuses on a discussion of coupled hydromechanical (HM) processes in these three formations, pointing out issues common to all of them. We submit that an understanding of such coupled processes in all three formations provides a deeper insight and thus a higher confidence in our knowledge concerning this area of research. Further, lessons learned from investigations in one formation may teach us how to approach the problem in another formation.

In the next section, a general discussion is provided on the key issues and associated parameters related to coupled HM processes in crystalline rock, plastic clay and indurated clay. Following this discussion, one particular type of HM coupling studied in all three formations is specifically discussed as an example. This is the problem of pore water pressure changes in the rock next to a tunnel during excavation using a tunnel boring machine (TBM). Field investigations conducted in the three formations are described. Lessons learned from the three studies are comparatively discussed and potential cross-fertilization of ideas is proposed.

2. COUPLED HM PROCESSES IN CRYSTALLINE ROCK, PLASTIC AND INDURATED CLAYS

It is interesting to note that the three rock types all have an undisturbed flow permeability of about 10^{-19} to 10^{-20} m^2. For crystalline rock, this range represents the permeability of the rock matrix, i.e. without fractures. Crystalline rock contains a network of naturally occurring fractures, so that its measured effective permeability is, depending fracture distribution

and connectivity, about 10^{-17} to 10^{-19} m^2. With stress release accompanying tunnel excavation, the increase in permeability in crystalline rock is one or two orders of magnitude, i.e., a resulting permeability of about 10^{-15} to 10^{-17} m^2 (EC 2005), which happens to be similar to the measured values for EDZ in plastic or indurated clays immediately after tunnel excavation (EC, 2005; Bastiaens et al., 2006).

Tables 1a and 1b present a comparative summary of the underlying physical processes and key property parameters for HM couplings in the three rock types under, respectively, stress changes and water content changes.

Table 1a. Comparison of processes and parameters in different rock types: under stress changes (e.g., stress release due to tunnel opening)

	Crystalline Rock	Plastic Clay	Indurated Clay
Processes and Events	Stress redistribution due to opening, causing tension, compression and shear in different parts around the drift. Progressive failure and spalling. Transient pore-pressure dissipation.	Stress release at excavation (stress redistribution) leading to contractant and dilatant processes with induced fracturing. Shear deformation also expected. Undrained behaviour in the short term. Dilation inducing suction and pseudo-strength increase. Transient pore-pressure dissipation.	Stress redistribution and material anisotropy leading to (a) tensile and shear failure along bedding planes and (b) extensional or tensile fracturing tangential to the tunnel walls. Progressive failure and spalling. Undrained behaviour in the short term. Transient pore-pressure dissipation.
Property Parameters	State of *in situ* stress and pore pressure. Elastic properties of the rock. Rock strength (failure initiation strength). Heterogenity of rock parameters. Initial *natural* fracture network (density and orientations).	State of *in situ* stress and pore pressure. (Non-linear) elastic properties of the rock. Biot coefficient and Skempton factor. Rock compaction and overconsolidation ratio. Rock strength (failure initiation strength). Heterogenity of rock parameters. Natural fractures observed in outcrops with spacing 0.5 to several meters (mostly extensional fractures with a small part shear fractures) are not detected at depth. Confining pressure, as well as moisture content, is reason for absence of fractures. Presence of bedding planes. Moisture content in rock and transient pore pressure.	State of *in situ* stress and pore pressure. (Non-linear) elastic properties of the rock including their anisotropy (bedding planes). Biot coefficient and Skempton factor. Rock compaction and overconsolidation ratio. Rock strength (failure initiation strength). Heterogenity of rock parameters. Initial *natural* fracture network (density and orientations). Moisture content in rock and transient pore pressure (medium characterized by dependence on moisture content: lower moisture content leads to stiffer and more brittle rock).

Table 1b. Comparison of processes and parameters in different rock types: under hydraulic changes (e.g., dehydration due to tunnel ventilation)

	Crystalline Rock	Plastic Clay	Indurated Clay
Assumed Condition	Open and unsupported tunnels	Massive tunnel lining from prefabricated cement blocks (wedge block technique)	Open tunnels with support by rock bolts and mesh
Processes and Events	Hydraulic pressure changing effective stress, inducing fracture deformation. Air entry resulting in oxidizing conditions, two-phase flow conditions (effective water conductivity decreased). Potential chemical and bacterial activities with possibility of clogging against flow.	Drainage into the tunnel leads to increase in effective confining stress. Suction development on the wall due to dilatancy (induced consolidation), which may strengthen the rock. Pressure on liner causes a transition from dilatant to contractant regime in the EDZ; creep and possible fracture closing. Drift ventilation and rock dehydration changing clay properties; ventilation retards self sealing.	Drainage into the tunnel leads to increase in effective confining stress. Air entry resulting in oxidizing conditions, two-phase flow conditions (effective water conductivity decreased). Oxidation of pyrites-production of sulfuric acid. Ventilation de-saturateses the rock leading to significant suction pressure which may strengthen the rock but may also lead to extensional (drying) fractures normal to the tunnel wall. Rock creep rates in the tunnel near field may directly be controlled by rock de-saturation. Potential microbiological processes.
Property Parameters	Changes in fluid pressures. Humidity condition and its variation. Fracture apertures and porosity. Fracture density.	Changes in fluid pressures. Humidity condition and its variations. Suction as a function of dilatancy. Changes of rock strength and deformation behaviour due to de-saturation and compaction.	Changes in fluid pressures. Humidity condition and its variations. Suction as a function of de-saturation. Changes of rock strength and deformation behaviour due to de-saturation and compaction. Effect of heterogeneity in rock property (clay content and hence rock strength not uniform). Geometry, apertures and density (connectivity) of induced fractures.

Crystalline rock and plastic clay form end members of different material classes. While crystalline rocks are nearly perfect brittle material, the plastic clays can be described as ductile or visco-elasto-plastic materials. However, around the excavation a brittle behaviour is also observed in plastic clays due to the suction development. In contrast, indurated hard clays are transitional materials, which, depending on their water content may behave brittle (low water content) or ductile (high water content). A careful perusal of Tables 1a and 1b finds that there are many common factors and parameters that play a key role in the coupled HM processes in all three rock

types. Thus, stress release due to tunnelling in crystalline rock causes extension, compression, and shear in different parts around the drift (Table 1a). These effects interact with the rock fracture network, and, depending on the anisotropy of the *in situ* stresses and rock strength, may cause fracture opening or closing as well as fracture initiation. The fracture creation, propagation or alteration would have a major impact on fracture hydraulic conductivity. Since the process is intrinsically anisotropic, its hydraulic impact will also be anisotropic. These discussions are also applicable to indurated and plastic clays, except in these cases there may be no pre-existing fracture networks, dependant on the site, but new fractures can be induced especially along bedding planes or planes of weakness and impurities. The physical processes are similar, though parameters are quite different. In particular, clay involves large deformations, so that the simple small-deformation constitutive equations useful for crystalline rocks will need to be modified and improved.

On the one hand, with the tunnel representing a hydraulic sink, the hydraulic changes in crystalline rocks increase or reduce the effective stress, with resulting fracture-aperture and permeability changes (Table 1b). On the other hand, tunnel ventilation dehydrates the rock near the tunnel, and the air entry into the rock results in two-phase flow conditions with reduced effective hydraulic conductivity. For plastic and indurated clays, tunnel ventilation and rock dehydration significantly change rock strength parameters. The rock creep and self-sealing effect, occurring in the clay formations (and not in crystalline rocks), is a strong function of the water content. Note, in particular, that indurated clay behaves like a soft clay at high water content, but at low water content behaves like a brittle rock with micro-cracks and macrofractures, created along bedding planes or planes of heterogeneity.

Below, we shall present a comparative discussion of one hydromechanical coupling in the three rock types — the pore pressure change in the nearby rock during tunnel excavation using a TBM. This process has been a topic of investigation in major field experiments in recent years. They are described in the following three sections for crystalline rock, plastic clay, and indurated clay, respectively. After these three sections, a comparative discussion of lessons learned and key issues will be presented.

3. PORE PRESSURE CHANGES DURING TUNNEL DRILLING IN CRYSTALLINE ROCK

During the excavation of the FEBEX Tunnel, located in fractured crystalline rock at the Grimsel Test Site in Switzerland, peculiar responses in fluid pressure were observed in the surrounding rocks (McKinley et al., 1996). A borehole was first drilled at 3 m parallel to a planned tunnel and then packered into two 10-m sections, P3 and P4. During tunnel drilling using a TBM, the water pressures in P3 and P4 were monitored. The front end of the tunnel passed P4, but just reached P3. Thus the pressure behavior in P3 was not so clear, as one would expect, but the P4 pressure showed a distinct response, with two peaks corresponding to two drilling-and-resting cycles (Figures 1 and 2). It is believed that during tunnel drilling directly across from P4 interval, the pore pressure in P4 increased because of the induced stress concentration near P4. Then, during the resting period between drilling, water leaked away because of rock permeability, and thus the pore pressure decreased (Figure 2).

To understand the data, a fully coupled three-dimensional HM modeling of the tunnel-drilling procedure was performed (Rutqvist et. al., 2004) using a finite element code ROCMAS (Rutqvist et al., 2001). The material properties of the rock mass used are given in Table 2. An initial stress field was assigned according to the range of stress measurements in the Grimsel area (Pahl et al., 1989): σ_v=10 MPa, σ_h=15 MPa and σ_H=30 MPa, where σ_H is oriented 45º from the tunnel axis.

The FEBEX tunnel was modelled according to the actual TBM schedule. The boring was conducted in ten-hour shifts with no activities during nights and weekends, and, in the modelling, uniform excavation during each ten-hour shift is assumed. Figure 3 presents the simulated changes in mean stress at the end of Section-3 excavation (Figure 2). Figure 4 shows the corresponding fluid pressure, with two zones of increased values, one around the front-left side of the excavation and one above it, near its front. Figure 3 shows that near these two zones of pressure increase, the mean stress has increased as a result of the excavation. In contrast, the fluid pressure on the side of the drift is decreased where the mean stress has decreased. The figures also show that the HM-induced changes in fluid pressures are temporal. For example, the HM-

induced fluid-pressure rise above the tunnel diminishes 5 to 10 m behind the tunnel face, because of drainage into the tunnel.

Figure 5 presents the predicted and measured pressure responses in P4. While the timing of pressure response is about right, the predicted values are opposite to what were measured, i.e., pressure drops instead of peaks. The reason behind the discrepancy was found in the assumed *in situ* stress field, which is an important factor that controls the fluid-pressure changes. Employing a variation study, it was found that the measured pressure changes can be reproduced by changing the orientation and magnitude of the stress field. An example of a much-improved match is shown in Figure 6, together with the adjusted stress field shown in the upper-right corner. The main point of this example is to show the high sensitivity of pore pressure changes to local *in situ* stress field.

It was shown in a more general study that the measured pressure responses can be captured if the stress field is rotated such that contraction (compressive strain rate) and corresponding increases in mean stress occur near the P4 borehole on the side of the drift. Good agreement between measured and simulated evolution of fluid pressure could be obtained if the maximum principal stress were rotated about 40° from the horizontal. Such a rotation of the local in situ stress field is not unrealistic, especially considering the presence of the Lamprophyre zones and other geological features.

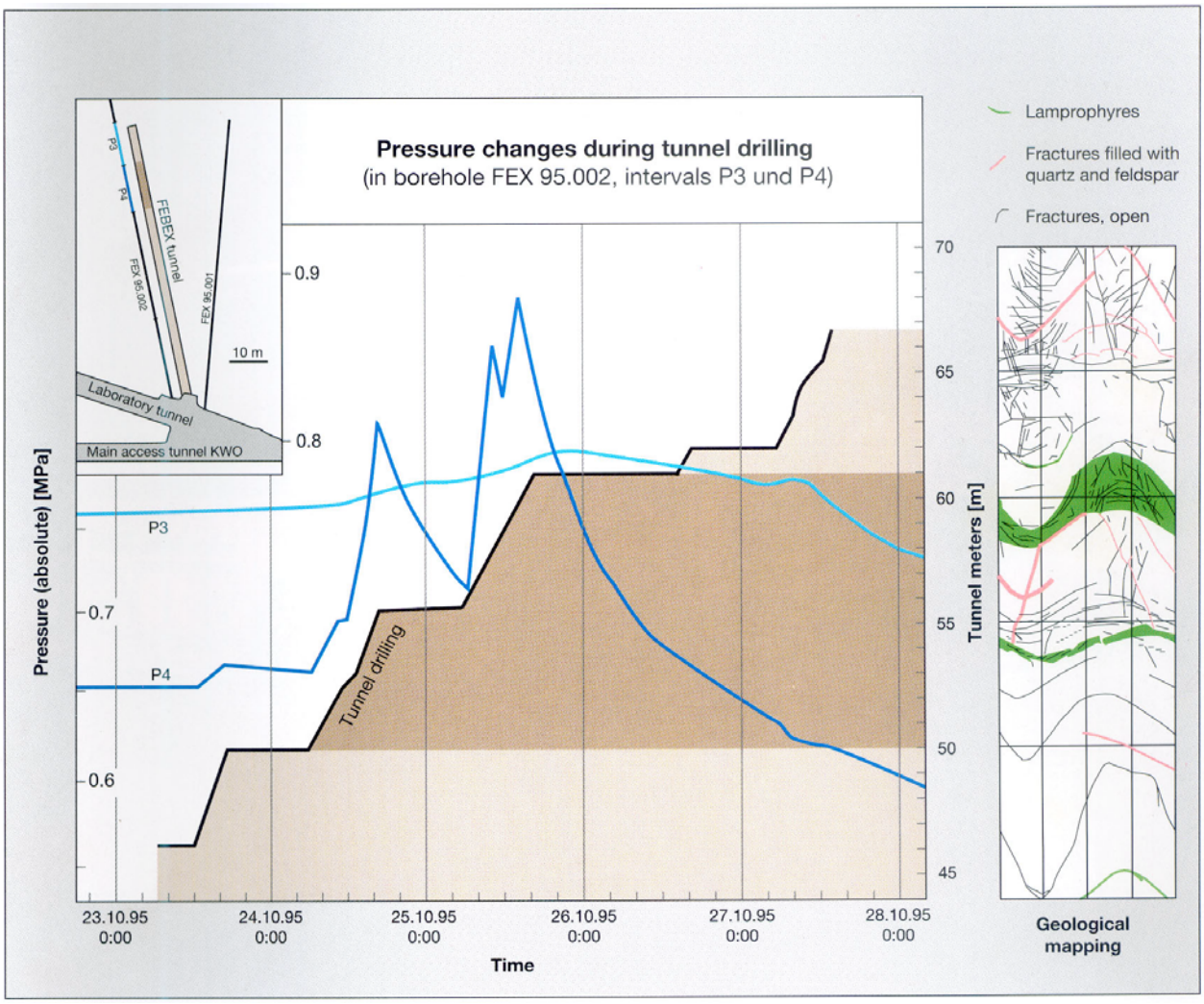

Figure 1. During tunnel-boring-machine (TBM) excavation of the FEBEX tunnel, distinct increases in fluid pressure were observed in a borehole interval (P4) located a few meters away from the drift wall (from McKinley et al., 1996).

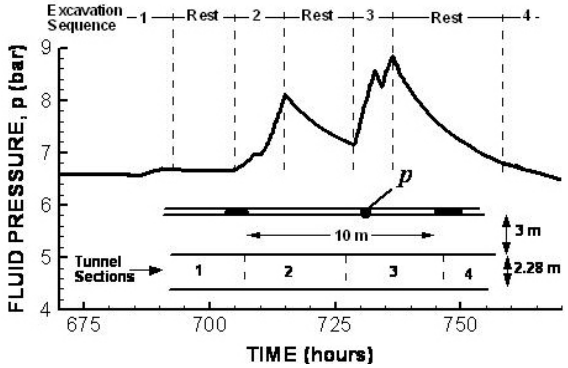

Figure 2. Pore pressure in borehole interval P4 during tunnel excavation.

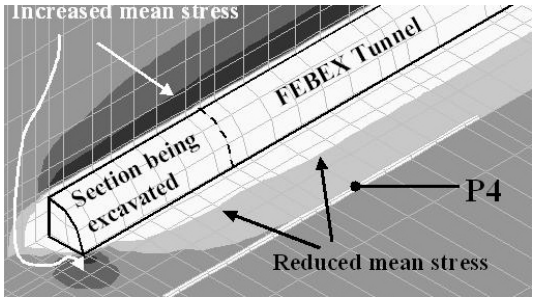

Figure 3. Calculated changes in mean stress at end of excavating Section 3 of the FEBEX tunnel (see Figure 2) (from Rutqvist et al., 2004).

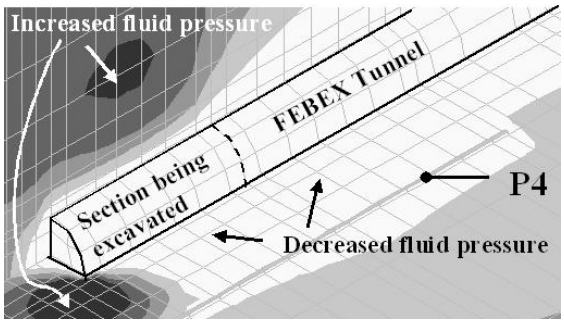

Figure 4. Calculated change in pore pressure at the end of excavating Section 3 of the FEBEX tunnel (see Figure 2) (from Rutqvist et al., 2004).

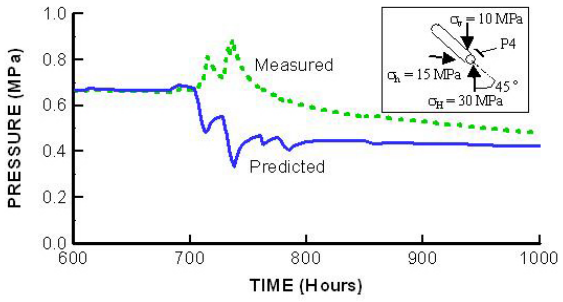

Figure 5. Predicted and measured pore pressure evolution for the estimated regional stress field (from Rutqvist et al., 2004)

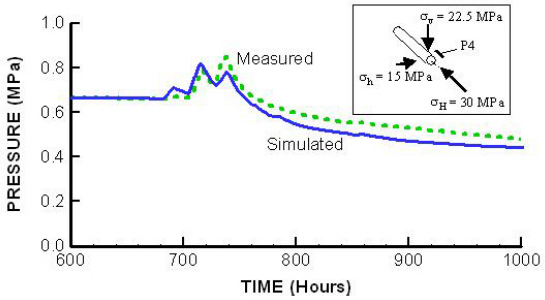

Figure 6. Simulated and measured pore pressure evolution for the adjusted local stress field (from Rutqvist et al., 2004)

Table 2. Properties for FEBEX site

PARAMETER	VALUES
Porosity	0.01
Young's modulus	35 GPs
Poisson's ratio	0.3
Vertical permeability	5×10^{-18} m^2
Horizontal permeability	5×10^{-19} m^2
Lamprophyre permeability	1.10×10^{-17} m^2

4. PORE PRESSURE CHANGES DURING TUNNEL DRILLING IN PLASTIC CLAY

The underground research facility HADES (High-Activity Disposal Experimental Site), at Mol, Belgium, at a depth of 223 m in a plastic clay formation ("Boom Clay"), was constructed to allow various *in situ* experiments for evaluating the feasibility of high-level radioactive waste disposal in such formations. The first construction phase of the HADES facility was started in 1980 and then expanded several times (Figure 7). Of particular interest to the present discussion is the construction of the "Connecting Gallery" in 2001–2002 (Bastiaens et al., 2003; Bastiaens and Bernier, 2006). Prior to the drilling of this tunnel, a series of instrumented boreholes A, B, C, D, and E were established under the CLIPEX (Clay Instrumentation Program for the Extension of an Underground Research Laboratory) project (Bernier et al., 2002). These allowed the monitoring of pore pressure, total stress, and displacement before and during the construction of the Connecting Gallery (Figure 8).

During drilling of the Connecting Gallery (at 3 m/day), pore pressure responses were noticed many meters into the rock around the tunnel being

drilled. Figure 9 shows the pore pressure response in borehole B2, which is in front of the drilling (i.e., drilling is towards the borehole; see Figure 8) and in borehole E2, which is parallel to and 4.1 m above the external boundary of the Connecting Gallery which was being drilled (Figure 8).

In Figure 9 top, the different curves correspond to different packed intervals in borehole B2, with their initial pore pressures being slightly different from each other because of their distances from the Test Drift. Changes in pore pressure were noticed up to 60 m ahead of the drilling front of the Connecting Gallery. They increased to a peak when the tunnel face was about 10 m from the sensors, and then dropped quickly to atmospheric pressure. This can be understood from the low permeability of the clay ($2–4 \times 10^{-19}$ m^2) and the high rate of excavation (~3 m/day), so that the excavation can be considered as under an undrained condition, with pore pressure rising on account of the stress-induced deformation in the clay mass. The drop of pore pressure as the drilling front approached very close to the sensors can be due to excavation-induced fractures in the rock in front of the drilling face, created by the local high decompression of the rock mass. This is confirmed by the pore pressure changes shown in Figure 10, which shows a sudden pressure-equilibrium with the atmosphere in the rock at about 2–3 m ahead of the drilling face.

In Figure 9, bottom part, the pore pressure response in borehole E2 is shown together with the displacement, as the Connecting Gallery is drilled parallel to it. The pressure response and mechanical displacement are well coupled. Note that the pressure and displacement becoming steady as drilling passed the sensors could be a result of the emplacement of lining support following the drilling front.

Numerical simulation of these data has been conducted (Li et al., 2006), and some of the property parameters used are shown in Table 3. The results show that pore pressure evolution calculated by assuming a Mohr-Coulomb model agrees well with the general tendency of the data, but cannot reproduce the extent and magnitude of the pore pressure changes ahead of the drilling front. It is likely that a more sophisticated constitutive law, such as that of Kaliakin and Dafalias (1990), is needed to properly account for the progressive transition of elasto-plasticity of plastic clay. Other factors that may play a role are the *in situ* stress field and clay property anisotropy.

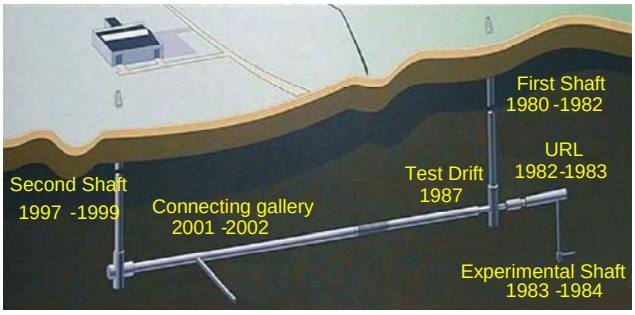

Figure 7. Underground research facility, HADES, at the Mol site (from Bastiaens et al., 2003). The distance between the First and the Second Shaft is 157 m.

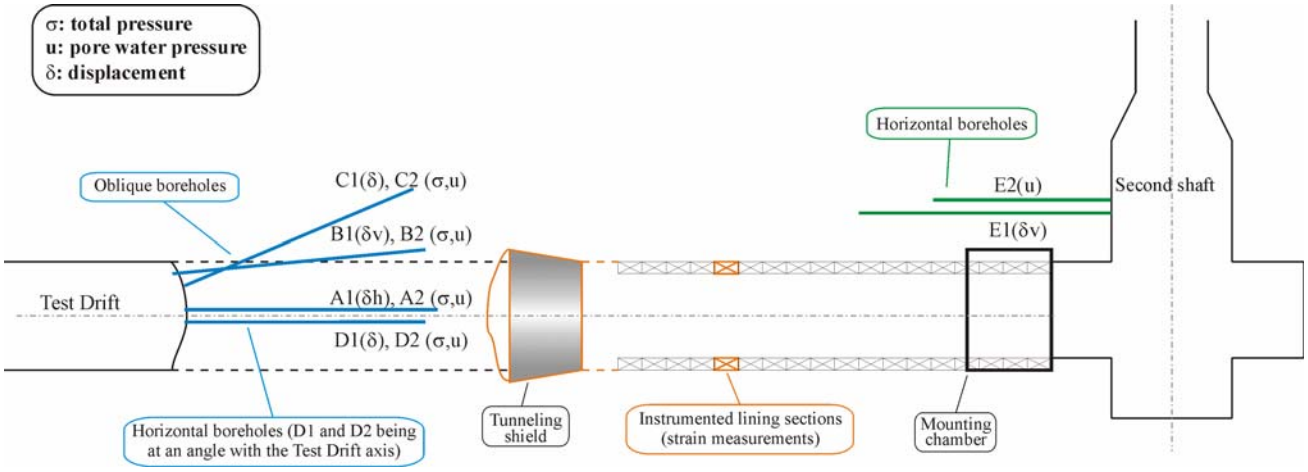

Figure 8. CLIPEX instrumentation program in boreholes A, B, C, D, and E. Note that this figure corresponds to the left-right reverse of Figure 7 (from Bastiaens et al., 2003). The distance between Second Shaft and Test Drift is 90 m.

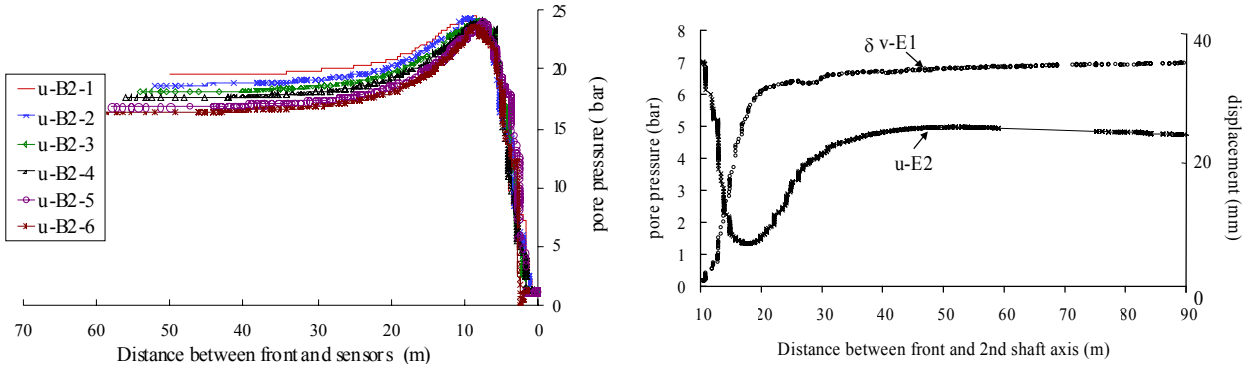

Figure 9. Upper figure shows pore pressure (u) evolution in Borehole B2; lower figure shows pore pressure (u) and displacement (v) in Borehole E2 and E1 (from Bastiaens et al., 2003).

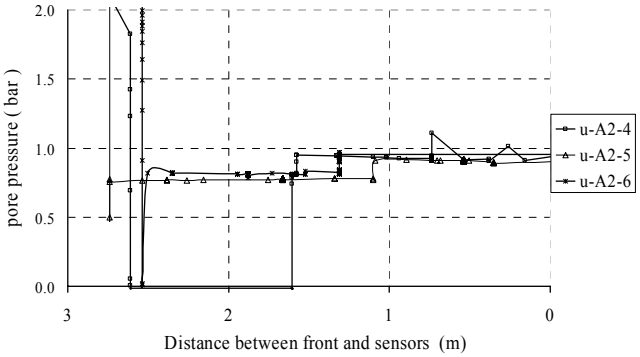

Figure 10. Pore pressure in borehole A3 showing evidence of fracturing (from Bastiaens et al., 2003)

Table 3. Drained property parameters for Boom Clay (Li et. al., 2006)

Young's modulus	300 MPa
Poisson's ratio	0.125
Friction angle	18º
Cohesion	0.3 MPa
Dilation angle	0º
Saturated permeability	4×10^{-19} m^2
Porosity	0.39

5. PORE PRESSURE CHANGES DURING TUNNEL DRILLING IN INDURATED CLAY

Marschall et al. (2006) reported a recent field study of pore-pressure changes due to tunnel excavation in indurated clay. A horizontal micro-tunnel (13 m long and 1.036 m diameter) was drilled in an overconsolidated claystone (Opalinus Clay) formation in the Mont Terri Underground Rock Laboratory in the Jura Mountains, Switzerland. The indurated clay has low permeability (~2×10^{-20} m^2), a self-sealing capacity, low rock strength, and anisotropic geomechanical properties, with much of its properties sensitive to water content and saturation. It is highly fractured, but the fractures are generally tight for the in-depth stress conditions. Property parameters are summarized in Table 4.

Before excavation of the microtunnel, 12 boreholes (HG-A2 to HG-A13) were emplaced and instrumented (Figure 11). In HG-A2 and HG-A3, hydraulic triple packer systems were emplaced for pore pressure measurements. The triple packer system separates each of the boreholes into three monitoring intervals, labeled "-i1", "-i2" and "-i3", corresponding to, respectively, 14–12.5 m, 12–9.5 m, and 9–5.5 m along the borehole.

Figure 12 shows the pore pressure evolution in the monitoring intervals in HG-A2 and HG-A3 during tunnel excavation (at 1.5 m per hour). Pore pressure changes in HG-A2 (lower three curves in Figure 12) are significantly smaller than those in HG-A3 and exhibit some anomalous behavior. This behavior can be explained by HG-A2 being significantly farther from the tunnel than HG-A3 and experiencing a higher "de-stress" because of the excavation directly below it. Further, a hydraulic communication between monitoring intervals A2-i1 and A2-i2 was detected immediately after packer inflation. For these reasons, let us mainly consider the pore pressure evolution in BHG-A3 (upper three curves in Figure 12).

Before excavation, pore pressure in HG-A3 ranged between 0.75 and 0.9 MPa. Immediately after excavation was initiated, a significant rise was seen in all three monitoring intervals. The step-wise drilling procedure used was reflected in the pore pressure increases during this time. After termination of tunnel excavation, pore pressure continued to increase to a peak of 2.1, 1.9, and 1.75 MPa in intervals A3-i3, A3-i2, and A3-i1, respectively. Three weeks after excavation ended, pressures started to decrease steadily, a trend still ongoing at the time of the Marschall et al. paper (February 2006). The steady decrease of pore pressure over the last year may not be related to the microtunnel, but to the growing cone of depression due to pore water drainage into the nearby Gallery 2004 (Figure 11).

The pore pressure increase during excavation can be explained by rock compression under undrained conditions due to the immediate reaction on the stress redistribution, as with plastic clay or crystalline rock, while the continued increase for three weeks after termination of excavation may be due to progessive failure processes in the tunnel near-field and a time-dependent growth of the EDZ, leading to continous redistribution of stresses until a semi-stable equilibrium is reached. Monitoring of deformations and pore pressures in all 12 observation boreholes suggested a quasi-continuous evolution of the damaged zone around Gallery 2004 and the microtunnel, including

strength degradation of the rock because of the varying ventilation conditions. Tunnel ventilation created extended desaturation joints when the humidity inside the tunnel was low and caused rock softening when the humidity was high. Further studies of these effects, including numerical modeling efforts, are under way (Marschall et al., 2006).

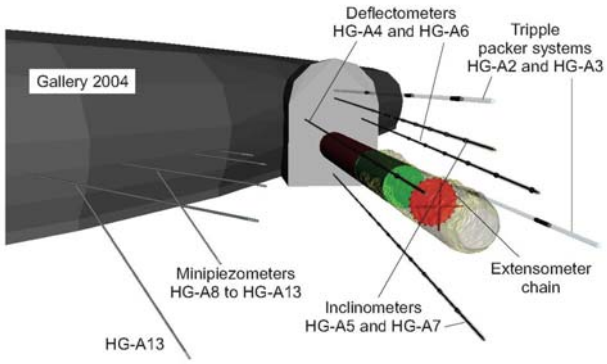

Figure 11. The site for the microtunnel in the Mont Terri Underground Rock Laboratory, showing its 12 monitoring boreholes (from Marschall et al., 2006).

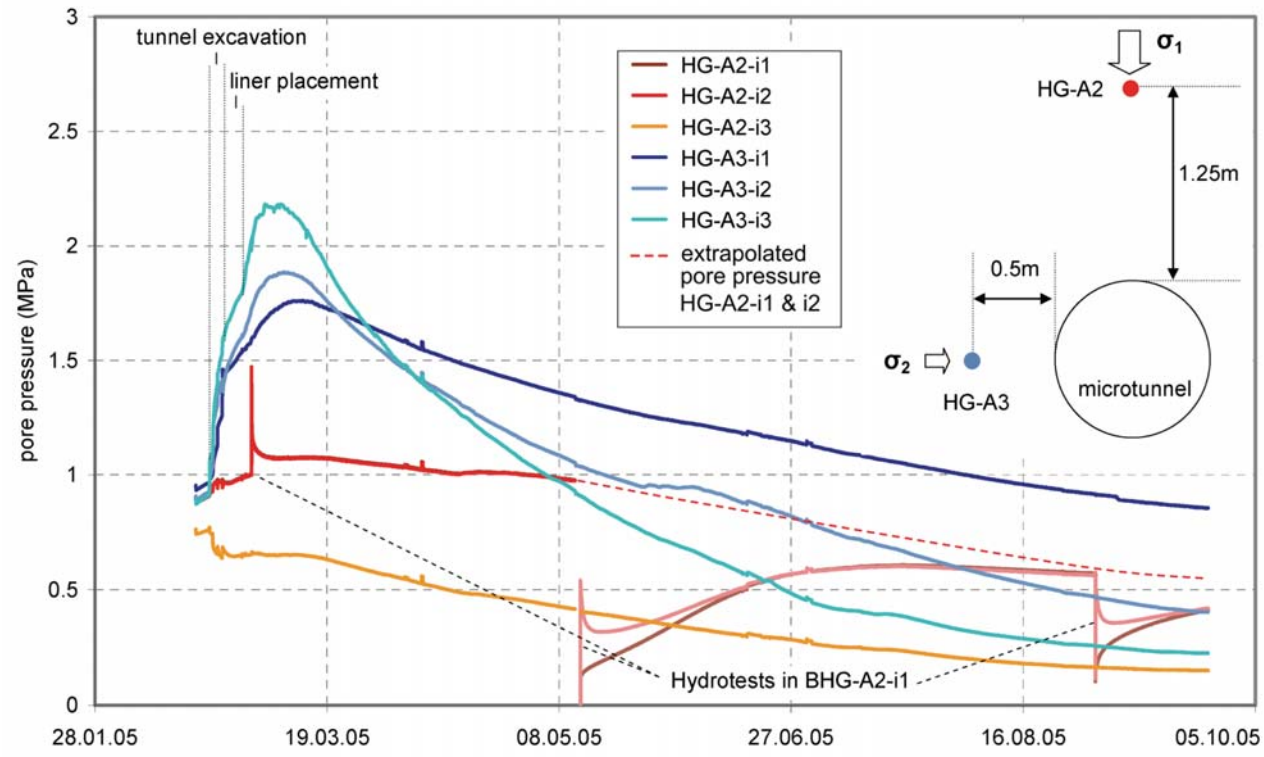

Figure 12. Pore pressure evolution in the three packed intervals in boreholes HG-A2 and HG-A3 (from Marschall et al., 2006). The top three curves correspond to data from HG-A3.

Table 4. Geotechnical reference parameters of the Opalinus Clay at the Mont Terri Underground Rock Laboratory. Parameters of the bi-linear Mohr Coulomb model after Blümling and Konietzky, 2004.

Parameter	Matrix	Bedding
Hydraulic permeability (m^2)	2×10^{-20}	
Poisson's ratio [-]	.027	
Bulk density [kg/m^3]	2450	
Porosity	0.156	
Bulk modulus (drained) [MPa]	2000	
Bulk modulus (undrained) [MPa]	8400	
Tensile strength [MPa]	1	0.5
Peak cohesion [MPa]	3.0[a]/14.6[b]	1.0[a]/7.7[b]
Peak friction angle [º]	39[a]/14[b]	34[a]/12[b]
Residual cohesion {MPa]	1.5[a]/7.3[b]	0.5[a]/3.9[b]
Residual friction angle [º]	33[a]/12[b]	29[a]/10[b]
Assumption: Ubiquitous joint, bi-linear Mohr-Coulomb failure criteria with: [a]Normal stress < 10MPa [b]Normal stress .> 10 < MPa		

6. COMPARATIVE DISCUSSION OF PORE PRESSURE CHANGES IN THE THREE ROCK TYPES AND LESSONS LEARNED

The pore pressure changes caused by tunnel excavation in crystalline rock, plastic clay, and indurated clay are mainly controlled by the same physical processes, namely the early undrained compression of the rock mass, changing the pore size and thus the pore water pressure. Subsequent pressure recovery occurs as a result of water diffusion away from the pore through fractures, bedding planes, or rock matrix. The time scale is quite different, depending on the permeability of the rock mass and rock deformability. For example, the time scale for crystalline rock is much shorter than those of the plastic and indurated clays.

For the FEBEX Tunnel study in crystalline rock, the modeling study shows a high sensitivity to *in situ* stress field. Dependent on the magnitude and orientation of stresses, the pore pressure responses could be quite different, so that a calculated dip (decrease) in pore pressure could become a peak instead. This possibility points to the importance of the local stress field tensor, and also to the role of material property anisotropy. These factors should be considered in modelling the behavior in plastic and indurate clays.

For plastic clay, pore pressure changes cannot be reproduced using a Mohr-Coulomb model, and a more sophisticated constitutive relationship may be needed in order to properly describe the progressive transition of elasto-plasticity in plastic clay. Further investigation of this and other issues is under way.

For indurated clay, such as the Opalinus Clay at the Mont Terri Underground Facility, more complex processes seem to be at play. These may include influences of nearby galleries and material property changes caused by cyclic ventilation with associated dehydration and rehydration. It is still unclear whether these are the controlling issues, or whether the field data can be explained by a careful modelling accounting for details of the drilling procedure and the installation of steel liner over the first half of the tunnel. Also, similar to the experience from the plastic clay case, a sophisticated constitutive material model including the effects of de- and rehydration may be needed. Considerable effort is currently underway to investigate these issues.

The comparative discussion of the same type of experiments in crystalline rock, plastic clay, and indurated clay, as presented above, serves to demonstrate that the main physical processes are common to all these cases, though with very different characteristic time constants. Lessons learned from one rock type may indicate issues to consider in the other two types, thus providing added opportunities for cross-fertilization. Understanding the results in all these cases, each with drastically different property parameters, will enhance considerably our confidence in the state of science regarding such coupled hydromechanical processes.

ACKNOWLEDGMENTS

The authors would like to thank many collaborators over the years in studies discussed in this paper. The first author would like to acknowledge helpful discussions with members of the DECOVALEX project, particularly Jonny Rutqvist, Ove Stephansson and John Hudson. The paper was prepared with partial support of U.S. Department of Energy under Contract No. DE-AC02-05CH11231 with the Lawrence Berkeley National Laboratory. Some results presented in the paper were obtained in the frame of the CLIPEX and SELFRAC projects. These projects

were co-funded by the European Commission within the fourth and fifth framework programmes, key action: Nuclear Fission. This support is gratefully acknowledged.

REFERENCES

Bastiaens, W., Bernier, F., Buyens, M., Demarche, M., Li, X.L., Linotte, J.-M., and Verstricht, J., 2003. The connecting gallery—The extension of the HADES Underground Research facility at Mol. Belgium. EURIDICE Report 03-294. Mol: EIG EURIDICE.

Bastiaens, W., and Bernier, F., 2006. 25 years of underground engineering in a plastic clay formation: The HADES underground research laboratory. In Bakker et al (eds.) *Geotechnical aspects of underground construction in soft ground.* London: Taylor and Francis group.

Bastiaens, W., Bernier, F., and Li, X.L., 2006. SELFRAC: experiments and conclusions on fracturation and self-healing and self-sealing processes in clays. *Applied Clay Science, Clays in Natural and Engineered Barriers for Radioactive Waste Confinement; Proc. Intern. Symp., Tours, 14-18 March 2005.* Amsterdam: Elsevier.

Bastiaens, W., Bernier, F., and Li, X.L., 2006. An Overview of Long-Term HM Measurements around HADES URF, Proceedings of EUROCK 06, European Regional ISRM Symposium, Multiphysics coupling and long term behaviour, Liège, May 9-12, 2006

Bernier, F., X.L. Li, J. Verstricht, J.D. Barnichon, V. Labiouse, W. Bastiaens, J.M. Palut, J.K. Ben Slimane, M. Ghoreychi, J. Gaombalet, F. Huertas, J.M. Galera, K. Merrien, and F.J. Elorza and Davies, C., 2002. CLIPEX: Clay Instrumentation Programme for the Extension of an Underground Research Laboratory, EUR 20619, Luxembourg: Commission of the European Communities..

Blümling, P., and H. Konietzky, 2004. Calibration and verification of a constitutive law for Opalinus Clay—Results from laboratory and *in situ* test, 2nd Colloquim "Rock Mechanics—Theory and Practice", March 2004, *Mitteilungen für Ingenieurgeologie und Geomechanik* (6). P. 89-95, Vienna.

EC (European Commission), 2005. CLUSTER EDZ, Impact of the Excavation Disturbed or Damaged Zone (EDZ) on the performance of radioactive waste geological repositories. Proceedings of an EC CLUSTER Conference and Workshop, Luxembourg, 03-05 November 2003, Nuclear Science and Technology, EUR 21028 EN, 2005.

Kaliakin, V. N. and Dafalias, Y. F., 1990. Theoretical aspects of the elastoplastic-viscoplastic bounding surface model for cohesive clays. Soils and Foundations, 30 (3): 11-24.

Li, X.L., Bastiaens, W., and Bernier, F., 2006. The hydromechanical ehaviour of the Boom Clay observed during excavation of the connecting gallery at Mol site. *Multiphysics coupling and longterm behaviour in rock mechanics; Proc. Intern. Symp., Liege, 9-12 May 2006.*

Marschall, P.; Distinguin, M.; Shao, H.; Bossart, P.; Enachescu, Chr.; Trick, T., 2006. Creation and Evolution of Damage Zones Around a Microtunnel in a Claystone Formation of the Swiss Jura Mountains; Society of Petroleum Engineers (SPE), Int. Symp. and Exhibition on formation damage control, Lafayette (Louisiana), February 15-17, 2006

McKinley, L., Kickaier, W., del Olmo, C., and Huertas, F., 1996. *The FEBEX project: full-scale simulation of engineered barriers for a HLW repository.* NAGRA Bulletin No 27, NAGRA, Switzerland.

Pahl, A., 1989. Heussermann, St., Bräuer, V., and Gloggler, W., 1989. Grimsel Test Site. Rock stress investigations. NAGRA, NTB, 88-39E.

Rutqvist, J., Borgesson, L., Chijimatsi, M., Kobayashi, A., Nguyen, T.S., Jng, L., Noorishad, J., and Tsang, C.-F. 2001. *Thermohydromechanics of partially saturated geological media: governing equations and formulation of four finite element models.* Int. J. Rock. Mech. Min. Sci. 38(1) 105-127.

Rutqvist, J., Rejeb, A., Tijani, M., and Tsang, C.-F., 2004. Analysis of coupled hydromechanical effect during drilling of the FEBEX Tunnel at Grimsel. In *Coupled Thermo-Hydro-Mechanical-Chemical Processes in GeoSystems,* edited by O. Stephensson, J.A. Hudson, and L. Jing. Elsevier Geo-Engineering Book Series Volume 2. 131–136, Elsevier Publishers, Amsterdam, The Netherlands.